Research Article

Journal of PeptideScience

Received: 10 March 2010 Revised: 8 July 2010 Accepted: 17 August 2010 Published online in Wiley Online Library: 11 January 2011

(wileyonlinelibrary.com) DOI 10.1002/psc.1298

Epitope motif of an anti-nitrotyrosine antibody specific for tyrosine-nitrated peptides revealed by a combination of affinity approaches and mass spectrometry

Mihaela Drăguşanu, Brînduşa-Alina Petre and Michael Przybylski*

Nitration of tyrosine residues has been shown to be an important oxidative modification in proteins and has been suggested to play a role in several diseases such as atherosclerosis, asthma, lung and neurodegenerative diseases. Detection of nitrated proteins has been mainly based on the use of nitrotyrosine-specific antibodies. In contrast, only a small number of nitration sites in proteins have been unequivocally identified by MS. We have used a monoclonal 3-NT-specific antibody, and have synthesized a series of tyrosine-nitrated peptides of prostacyclin synthase (PCS) in which a single specific nitration site at Tyr-430 had been previously identified upon reaction with peroxynitrite [17]. The determination of antibody-binding affinity and specificity of PCS peptides nitrated at different tyrosine residues (Tyr-430, Tyr-421, Tyr-83) and sequence mutations around the nitration sites provided the identification of an epitope motif containing positively charged amino acids (Lys and/or Arg) *N*-terminal to the nitration site. The highest affinity to the anti-3NT-antibody was found for the PCS peptide comprising the Tyr-430 nitration site with a K_D of 60 nM determined for the peptide, PCS(424-436-Tyr-430NO_2); in contrast, PCS peptides nitrated at Tyr-421 and Tyr-83 had substantially lower affinity. ELISA, SAW bioaffinity, proteolytic digestion of antibody-bound peptides and affinity-MS analysis revealed highest affinity to the antibody for tyrosine-nitrated peptides that contained positively charged amino acids in the *N*-terminal sequence to the nitration site. Remarkably, similar *N*-terminal sequences of tyrosine-nitration sites have been recently identified in nitrated physiological proteins, such as eosinophil peroxidase and eosinophil-cationic protein.

Keywords: tyrosine nitration; affinity-mass spectrometry approaches; proteolytic epitope excision; 3-nitro-tyrosine antigen–antibody complex; FTICR-mass spectrometry

Introduction

Tyrosine nitration has recently found increasing interest as an oxidative post-translational modification in proteins that has been shown to occur both at physiological conditions and to play a role in pathophysiological processes associated with oxidative stress such as atherosclerosis [1,2], bronchio-alveolar diseases, Alzheimer's and Parkinson's disease, and diabetes [3–5]. Nitrations of tyrosine residues *in vivo* have been detected (i) upon reaction with peroxynitrite and other nitrating agents [6] and (ii) by enzymatic reaction catalyzed by specific heme-peroxidases [7]. Thus, nitration may occur under physiological conditions, but may be substantially enhanced at pathophysiological conditions; however, details of reaction pathways and biochemical mechanism(s) of tyrosine nitrations are presently unclear [6,7]. Tyrosine-nitrated peptides have been discussed as potential oxidative biomarkers with higher specificity than merely the characterization of overall nitration levels in proteins [3,4,7]. However, the identification and structural characterization of tyrosine nitrations have been a significant bioanalytical and methodological challenge, as pointed out in recent reviews [6–10]. Protein nitrations have been detected in previous studies using antibodies against 3-NT [11] and by immunoanalytical methods such as immunohistochemistry [12], immunoprecipitation, Western blot [13,14], and ELISA [15], which provide overall determinations of nitration levels. However, only a few studies on the specificity and properties of 3-NT-antibodies have been reported [11,15]. Identifications of tyrosine nitration sites have been obtained by MS, but even with the use of MS methods major problems may arise due to (i) the typically low nitration levels in biological proteins and (ii) the photochemical instability and decomposition of nitrated peptides under conditions of MALDI-MS analysis which severely hampers the identification of nitration sites in proteins [16,17]. In recent years, combined approaches using affinity and MS methods (termed affinity-MS), particularly selective proteolytic digestion ('epitope-excision') have been successfully developed and applied to the molecular identification and structural characterization of epitopes in biopolymer–ligand complexes and protein modifications [18–21]. Using the combination

* *Correspondence to: Michael Przybylski, Department of Chemistry, University of Konstanz, 78457 Konstanz, Germany.*
E-mail: michael.przybylski@uni-konstanz.de

Laboratory of Analytical Chemistry and Biopolymer Structure Analysis, Department of Chemistry, University of Konstanz, D-78457 Konstanz, Germany

Abbreviations used: *3-NT, 3-nitrotyrosine; Tyr, tyrosine; FTICR-MS, Fourier transform-ion cyclotron resonance mass spectrometry; MALDI, matrix-assisted laser desorption-ionisation; ESI, electrospray ionization; SAW, surface acoustic wave; KLH, keyhole-limpet-hemocyanine; SPPS, solid-phase peptide synthesis; NHS, N-hydroxysuccinimide; TBME, tert-butylmethylether.*

Journal of PeptideScience

of proteolytic affinity extraction and high-resolution MS with immobilized 3-NT antibodies, nitration sites and structures have been unequivocally identified *in vivo* in several eosinophil granule proteins, even at low levels of nitration [22].

High specificities have been reported for both enzymatic and non-enzymatic tyrosine nitrations in biological proteins; however, significant differences were observed in binding affinities of tyrosine-nitrated peptides to anti-3NT- antibodies [11,15] which prompted our interest in the examination of a possible specific epitope motif to 3NT-specific antibodies. Based on the previously identified nitration at Tyr-430 of PCS [17], several PCS peptides comprising sequence variations at the Tyr-430 nitration site, and nitrated peptides comprising other tyrosine-containing peptides of PCS(Tyr-421; Tyr-83) were synthesized by SPPS. Binding affinities and specificities of the nitrated PCS peptides to a monoclonal anti-3NT-antibody were determined by ELISA, SAW-biosensor analysis, and proteolytic digestion in combination with affinity-MS. The results revealed an epitope motif for tyrosine-nitrated sequences with highest binding affinity for peptides containing positively charged amino acids at the *N*-terminal sequence to the nitration site, suggesting a corresponding motif as a basis for stabilization of tyrosine nitration sites in proteins.

Materials and Methods

Chemicals

The mouse monoclonal anti-3-NT antibody (MAB5404) employed was obtained from Chemicon International (Bubendorf, Switzerland) and was produced by using nitrated KLH as an immunogen. *N*-α-Fmoc-3-nitrotyrosine, *N*-α-Fmoc-protected amino acids, and PyBOP activator used for peptide synthesis were obtained from Bachem (Bubendorf, Switzerland). NHS-activated 6-aminohexanoic acid-coupled Sepharose was obtained from Sigma (St Louis, MO, USA). Micro-columns (0.2 ml) were obtained from Mobitec (Göttingen, Germany). Enhanced Chemiluminescence (ECL)-Western-blotting reagents were from Amersham (Mainz, Germany), TGA and TGR resin were from NovaBiochem (Laufelfingen, Switzerland).

Synthesis and High-Performance Liquid Chromatography of Nitrated PCS Peptides

Tyrosine- and 3-NT-containing peptides were synthesized on a semi-automated peptide synthesizer (EPS-221, Intavis, Langenfeld, Germany) by SPPS using Fmoc/*t*-butyl protection chemistry. Peptides with free carboxylate and amidated *C*-terminal were synthesized with TGA and TGR resin, respectively, using 40-min coupling and 5-min deprotection in 20% piperidine solution in DMF. Fmoc groups were removed from the Fmoc-protected resin prior to the first coupling cycle for 30 min at 25 °C. Cleavage and deprotection of the peptide from the resin was performed for 3 h at 25 °C trifluoroacetic acid/triethylsilane/water (95 : 2.5 : 2.5, v/v/v), and the crude peptide precipitated with 40 ml TBME at −20 °C. The resin and crude peptide were separated by filtration, and the peptide was frozen with liquid nitrogen and lyophilized. Peptides were purified by RP-HPLC using a Waters-Millipore (Eschborn, Germany) HPLC system with a M600A/M45 pump, 490E multi-wavelength detector and data system MAXIMA 820. Separations were carried out on a Vydac-C_{18}-column at a flow rate of 1 ml min^{-1} using a gradient elution system of 0.1% TFA (solvent A) and 0.1% TFA in acetonitrile: water 80 : 20 (v : v) (solvent B), 10–50%/50 min. Detection of tyrosine-nitrated and non-nitrated peptides was carried out at 365 and 220 nm, respectively (Figure 1(B)). Preparative purification was performed on a 250 × 20 mm preparative C_{18} column Grom-Sil 120 OSD-4 HE, 10 µm (Grom, Herrenberg, Germany) at a flow rate of 10 ml min^{-1} using identical eluent conditions as for analytical RP-HPLC.

Enzyme Linked Immunosorbent Assay

ELISA was performed in 96-well CovaLink-NH plates activated for 1 h at 25 °C with disuccinimidyl suberate solution (DSS) using 12 serial dilutions from 5 µM with the MAB5404 antibody. After overnight incubation at 25 °C, plates were washed four times with PBS-buffer and then blocked with two different blocking buffers (5% BSA, 0.05% Tween in PBS; and 0.1 M ethanolamine, 0.5 M NaCl pH 8.3), respectively, for 2 and 1 h. After washing with PBS-Tween, the plates were then incubated for 2 h at 25 °C with 100 µl per well antibody: BSA-Tween (1 : 3000), and unbound antibody removed with PBS-Tween. Plates were then incubated for 2 h with 100 µl mouse HRPAb: 5% BSA-Tween (1 : 5000) and unbound detection antibody removed by three washing steps with 200 µl per well PBS-Tween and one washing step with 200 µl per well citrate-phosphate buffer. Aliquots of 100 µl per well of substrate solution were poured into the wells of the CovaLink plate and the reaction monitored with a Wallac 1420- Victor2 ELISA plate counter at 450 nm.

Proteolytic Excision and Affinity-MS Methods

Immobilization of the MAB5404 antibody on NHS-activated sepharose was performed essentially as previously described [18,22]. Briefly, 100 µg of antibody was dissolved in coupling buffer (0.2 M $NaHCO_3$, 0.5 M NaCl, pH 8.3) and the solution added to dry NHS-activated 6-aminohexanoic-acid coupled sepharose and the coupling reaction performed for 2 h at 25 °C. The coupling product was loaded onto a 0.5 ml micro-column and washed sequentially three times each with buffer A (0.1 M ethanolamine, 0.5 M NaCl pH 8.3), buffer B (0.2 M CH_3COONa) and 0.5 M NaCl. The column was then stored at 4 °C in 5 mM NaH_2PO_4, 150 mM NaCl, pH 7.5, washed again with 20 ml PBS buffer and stored at 4 °C.

Epitope excision was carried out with 20 µg (10 µg $µl^{-1}$) of tyrosine-nitrated peptides subjected to the affinity column which was gently shaken for 1–2 h at 25 °C to allow complete binding of antigen. The supernatant was removed by blowing out of the column using a 10 ml syringe. The affinity matrix was washed with 60 ml PBS buffer for removal of unbound peptide, and the remaining affinity-bound peptide was digested for 2 h at 37 °C by addition of Trypsin (substrate: enzyme ratio, 50 : 1) in 200 µl PBS. Supernatant non-epitope peptide fragments were removed by blowing out of the column with a syringe, followed by washing the affinity matrix with 60 ml PBS buffer, until no background ions were detectable by ESI-MS. The immune complex was then dissociated by addition of 10 ml 0.1% TFA, and the eluate samples lyophilized and reconstituted in 0.1% TFA for MS analysis. The column was regenerated by extensive washing with PBS buffer.

Affinity-MS analysis was performed with 10 µg antigen peptides (µg $µl^{-1}$) in PBS buffer containing 5 mM Na_2HPO_4, 150 mM NaCl, pH 7.4 bound to the antibody column for 2 h. Unbound peptides were removed by washing with PBS, and the immune complex dissociated by addition of 0.1% TFA, pH 2. The washing and elution fractions were collected, lyophilized, redissolved in 0.1% TFA and desalted using the Zip Tip C_{18} procedure for ESI-MS

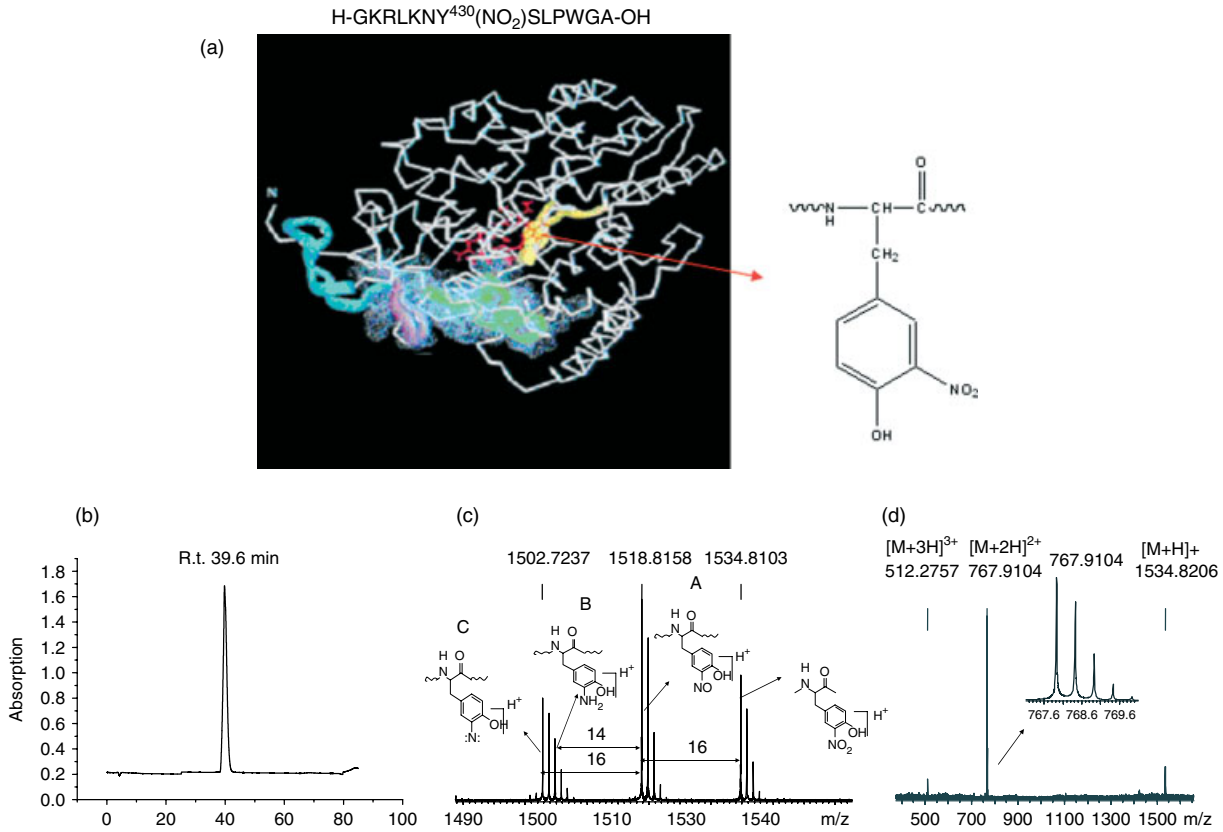

Figure 1. Tertiary structure of human PCS and characterization of synthetic tyrosine-nitrated PCS peptide. (A) Reconstructed 3D structural model of human PCS (PDB-ID, P450BM-3). Structural segments containing different tyrosine residues are highlighted by colored (blue, green, magenta) ribbons; the red arrow and structure denote the active site channel and heme, with the nitrated tyrosine-430 residue embedded in a tight fold around the heme-binding site [14]. (B)–(D) Characterization of tyrosine-430 nitrated peptide **5** PCS(424–436) by HPLC (B), UV-MALDI-MS (C), and nano-ESI-FTICR-MS (D). Photochemical fragmentation at the nitro-group in 5 is observed by UV-MALDI-MS.

analysis. Cross-reactivity of the column was tested with a series of tyrosine-nitrated and non-nitrated peptides (Table 1).

UV-MALDI and nano-ESI-FTICR MS was performed using a Bruker Daltonics APEX III Fourier transform ICR mass spectrometer (Bruker Daltonik, Bremen, Germany) equipped with a 7 tesla superconducting magnet, and external nano-ESI and MALDI ionization sources. 2,4-Dihydroxybenyzoic acid (DHB) was used as a matrix for MALDI-MS with the solvent, acetonitrile/0.1% TFA (1 : 1). ESI-ion trap-MS was performed with a Bruker Esquire 3000+ mass spectrometer (Bruker Daltonik) at the following conditions: capillary temperature, 200 °C; nebulizer gas, 20 psi (Ar); drying gas, 9 l min^{-1} (N_2); ESI source potential difference, 4 kV (positive ion mode); endplate offset, 500 V; skimmer, 40 V; capillary exit, 136 V. The ion trap was locked on automatic gain control, and six microscans were collected for each full MS scan with a maximum accumulation time of 200 ms for each ion.

Determination of Dissociation Constants

Dissociation constants were determined with an S-sens-K5 Biosensor instrument (SAW Instruments, Bonn, Germany) which is a chip-based bioaffinity system for marker-free detection of affinity-interactions based on the conversion of a high-frequency signal into a SAW due to the inverse piezoelectric effect [24,25]. The velocity of the SAW is sensitive toward changes in mass loading and viscosity causing shifts in the signal's amplitude and/or phase which enable sensitive detection on a gold-coated chip. Thus, interactions on the chip surface can be observed at near-physiological conditions. For measurements and calibration, the instrument was operated in the double-frequency mode, using five independent working channels on the chip [24]. A self-assembled monolayer (SAM) was formed on the gold surface by incubating a 10 mM solution of 16-mercaptohexadecanoic acid in chloroform for 12–14 h at 25 °C. After extensive washing of the chip surface, immobilization of peptide **5** (10 µM) was performed by activation using 50 mM NHS and 200 mM EDC, followed by buffer change to 5 mM Na_2HPO_4, 150 mM NaCl, pH 7.5. Antibody-association kinetics were determined by extracting the data from the sensor signals at all concentrations employed (1–100 nM), using the monomolecular growth model; the experimental decay model was used for determination of corresponding dissociation kinetics. The changes of sensor-phase signals were fitted with the program OriginPro 7.5 (OriginLab Coorporation, Northampton, USA) and FitMaster (Biosensor, Bonn, Germany); data were fitted for 1 : 1-Langmuir binding using

$$\Delta\varphi(t) = \Delta\varphi_{eq}[1 - \exp(-k_{obs}t)] \text{ for association and} \quad (1)$$

$$\Delta\varphi(t) = \Delta\varphi_{res} + [\Delta\varphi(t_{stop}) - \Delta\varphi_{eq}]\ \exp(-k_{diss}t) \text{ for dissociation} \quad (2)$$

$\Delta\varphi(t)$, phase shift at time t; $\Delta\varphi_{eq}$, phase shift at equilibrium; $\Delta\varphi_{res}$, phase shift of remaining ligand on surface; k_{obs}, pseudo-first order rate constant; $\Delta\varphi t_{stop}$, phase shift following dissociation.

Journal of PeptideScience

Corresponding fits were applied to the signals as shown in Figure 3, and the observed rate constant (k_{obs}) of the association phase plotted for each curve against the concentration, to extract K_D from the resulting linear regression line. Determination of the equilibrium dissociation constant is provided by

$$K_D = k_{off} k_{on}^{-1}. \quad (3)$$

Results

Synthesis and Structural Characterization of Tyrosine-nitrated Peptides of PCS

In a previous study, a specific nitration of PCS was identified upon reaction of bovine aortic microsomes with peroxynitrite at a single residue, Tyr-430, which is embedded in a tight fold around the heme-binding site of PCS [17]. Since the nitrated PCS showed high affinity to the 3-NT antibody MAB5404, Tyr-nitrated and non-nitrated peptides comprising sequence variations and partial sequences of PCS(421–439) were synthesized by SPPS using Fmoc protection [26] (peptides **5**–**17**; Table 1). The crude peptides were purified by preparative HPLC and characterized by nano-ESI-FTICR MS. HPLC characteristics and molecular ions of the PCS peptides are summarized in Table 1 (see also spectra in Figure 1(C) and (D)). It has been observed in previous studies of tyrosine-nitrated peptides by UV-MALDI-MS using the standard UV-N_2 laser at 337 nm, that photochemical decomposition occurs at the nitrotyrosine group [16], as illustrated in Figure 1(C) by the MALDI-FTICR-mass spectrum of peptide **5**. Fragment ions of 16 and 32 Da below the mass of the intact-nitrated peptide result from photochemical decomposition by loss of oxygen from the nitro-group to initially yield a nitroso-fragment, followed by loss of a second oxygen to form a nitrene-type fragment ion [16]. In contrast, ESI-mass spectra of tyrosine-nitrated peptides provide most abundant intact multiply protonated molecular ions without any detectable fragmentation (Table 1) [17,22].

Affinity-MS Characterization of Tyrosine-nitrated Peptides

Binding affinities of the tyrosine-nitrated and non-nitrated PCS peptides were initially characterized by affinity-MS [18], by affinity binding of peptides on the anti-3NT antibody column and subsequent MS analysis of eluted peptides, in order to characterize the specificity of the MAB5404 antibody. Figure 2 illustrates the analysis of a mixture of the nitrated and non-nitrated peptides PCS(424–439) (**5** and **6**) after incubation for 2 h on the antibody affinity column, followed by removal of non-binding peptides (supernatant fraction) and extensive washing with buffer. The immune complex was then dissociated with 0.1% TFA and the elution fraction characterized by ESI-MS. The affinity eluate showed exclusively the nitrated peptide **5** (Figure 2(A)). In a second experiment, an equimolar mixture of the Tyr-430- and Tyr-83-nitrated PCS peptides **5** and **3** were analyzed (Figure 2(B)). A significantly higher abundance in the affinity eluate was found for the Tyr-430 nitrated peptide **5**. This result suggested an effect of the amino acid sequence adjacent to the Tyr-nitration site on the binding affinity to the antibody (Figure 2(B)); thus peptide **5** contained basic amino acids *N*-terminal to the nitration site, while peptide **3** contained neutral and acidic residues.

Determination of Dissociation Constants of the PCS Peptide–Antibody Complexes

Quantitative affinity-binding studies of the nitrated peptides to the anti-3-NT antibody were performed with the SAW biosensor [24], after immobilization to a SAM on the gold chip surface. Peptide **5** (10 μM) was bound to the SAM and remaining active sites on the surface deactivated with 1 M ethanolamine and

Table 1. Structural and affinity characterization of tyrosine-nitrated and non-nitrated peptides of PCS

Peptide No.	Sequence	Nitration site	HPLC Retention time (min)	ESI-FTICR-MS[a] $m/z_{exp.}$	ESI-FTICR-MS[a] Δm (ppm)	Affinity[b] Dotblot
1	H-^{416}EKKDFY^{421}(NO_2)KDGKRL^{426}-OH	Y^{421}	28.2	1571.8075	6.4	+
2	H-^{416}EKKDFY^{421}KDGKRL^{426}-OH	–	32.5	1526.8298	2.3	–
3	H-^{79}DPHSY^{83}(NO_2)DAVVWEPR^{91}-OH	Y^{83}	27.5	1615.7130	1.2	+
4	H-^{79}DPHSY^{83}DAVVWEPR^{91}-OH	–	28.2	1570.7280	3.1	–
5	H-^{424}GKRLKNY^{430}(NO_2)SLPWGA^{436}-OH	Y^{430}	39.6	1534.8206	5.2	+
6	H-^{424}GKRLKNY^{430}SLPWGA^{436}-OH	–	32.7	1489.8270	4.6	–
7	H-^{424}AKRLKNY^{430}(NO_2)SLPWGA^{436}-OH	Y^{430}	36.5	1548.8230	3.2	+
8	H-^{424}GARLKNY^{430}(NO_2)SLPWGA^{436}-OH	Y^{430}	37.2	1477.7631	5.7	+
9	H-^{424}GKALKNY^{430}(NO_2)SLPWGA^{436}-OH	Y^{430}	38.1	1449.7565	5.5	+
10	H-^{424}GKRAKNY^{430}(NO_2)SLPWGA^{436}-OH	Y^{430}	37.7	1492.7770	7.7	+
11	H-^{424}GKRLANY^{430}(NO_2)SLPWGA^{436}-OH	Y^{430}	38.5	1477.7637	6.1	+
12	H-^{424}GKRLKAY^{430}(NO_2)SLPWGA^{436}-OH	Y^{430}	38.9	1491.8090	1.5	+
13	H-^{424}GKRLKNA^{430}SLPWGA^{436}-OH	–	33.6	1397.8059	3.3	–
14	H-^{427}LKNY^{430}(NO_2)-NH_2	Y^{430}	31.1	581.3071	4.0	–
15	H-^{427}LKNY^{430}(NO_2)SLP^{433}-NH_2	Y^{430}	31.7	878.4743	0.8	–
16	H-^{424}GKRLKNY^{430}(NO_2)SLP^{433}-NH_2	Y^{430}	32.5	1220.6831	6.5	+
17	H-^{421}YKDGKRLKNY^{430}(NO_2)SLPWGAGHN^{436}-OH	Y^{430}	37.4	2249.1320	4.6	+

[a] ESI-FTICR MS measurements were carried out with a 7T Bruker Daltonics APEX II FTICR mass spectrometer incorporating an external nano-ESI ionisation source [17].
[b] Affinity to the MAB5404 characterized by Dot blot; +, affinity to anti-3NT antibody; –, no affinity to anti-3NT antibody.

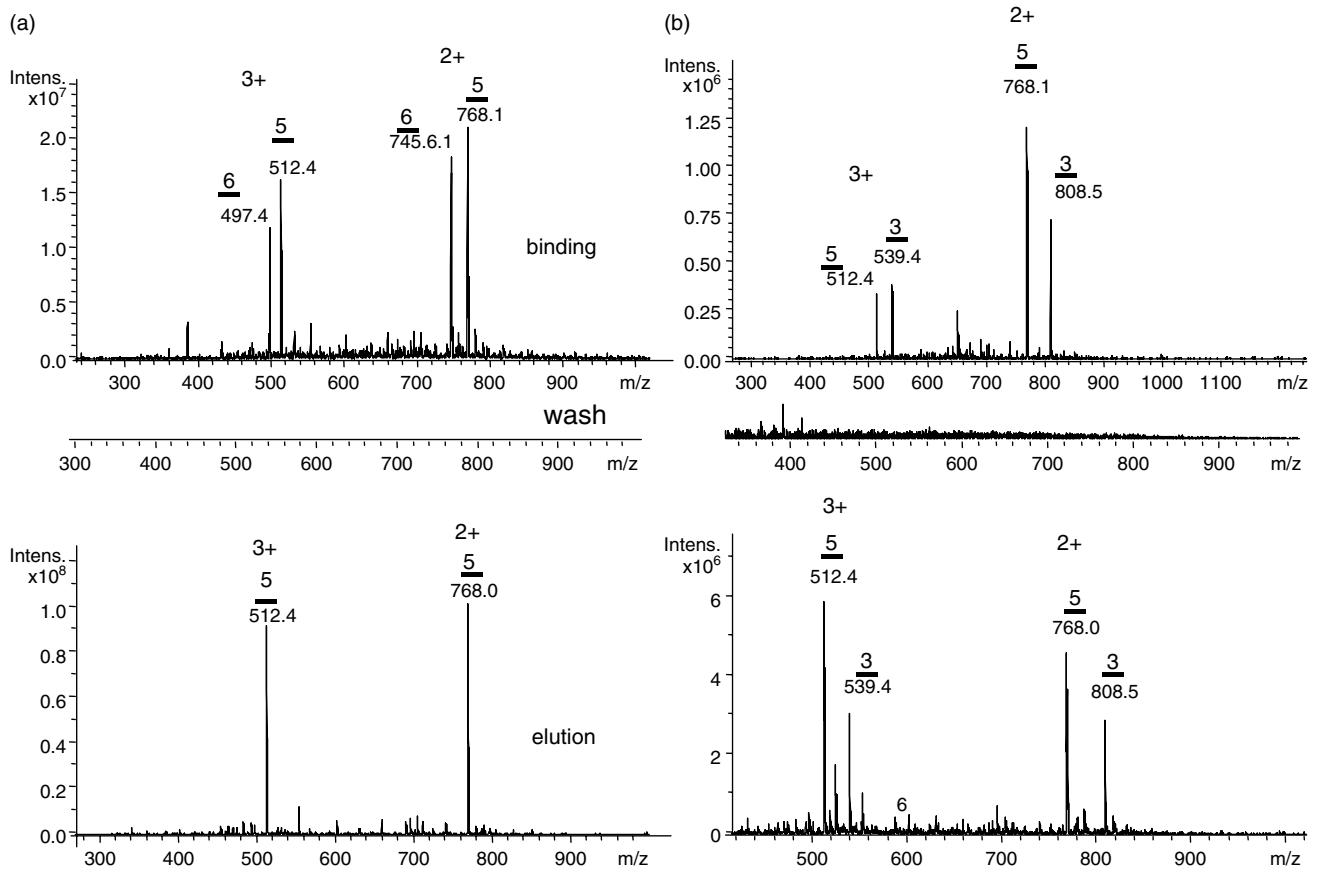

Figure 2. Affinity-MS analysis of binding of tyrosine-nitrated and non nitrated mixtures of PCS peptides to the antibody MAB5404: (a) ESI-MS of binding (supernatant), washing and elution fractions of a mixture of Tyr-430-nitrated peptide **5** and non-nitrated peptide **6** PCS(424–439); (b) binding and elution fraction of a mixture of Tyr-430-nitrated peptide **5** and Tyr-83-nitrated peptide **3**.

unspecific binding blocked by addition of anti-lysozyme antibody (500 nM; See Section on Materials and Methods). Following injection of increasing concentrations (10–100 nM) of the MAB-5404, binding curves were determined for peptide **5** (Figure 3(A)). Application of linear regression to the association kinetics and determination of the pseudo first-order constant k_{obs} from the biosensor signal–antibody concentration dependence provided k_{on} (2.1×10^{-5} $s^{-1}nM^{-1}$) and k_{off} values (1.3×10^{-3} s^{-1}), yielding a dissociation constant K_D of approximately 60 nM (Figure 3).

Epitope Motif of Tyrosine-nitrated Peptides to the Anti-3-NT Antibody

In order to identify a possible epitope motif for the tyrosine-nitrated PCS peptides to the anti-3NT antibody, affinity-binding experiments of the synthetic nitrated peptides were performed by trypsin digestion of the immobilized antibody–peptide complexes, followed by MS analysis of the eluted epitope-peptide fragments (epitope-excision; Figures 4 and 5) [18,19]. The Tyr-430 nitrated peptide **5** PCS(424–436) was bound to the antibody and the immobilized immune complex subjected to digestion with trypsin. Although the *N*-terminal sequence of the Tyr-430-nitrated peptide **5** contained two lysine and one arginine residues which are readily cleaved by trypsin without antibody binding, only the intact peptide **5** was isolated and identified in the affinity elution fraction. This suggested that the Lys-425, Arg-426, and Lys-428 residues were shielded by the antibody binding, and hence were considered to be part of the binding epitope. For further characterization of the binding epitope, the Tyr-430 nitrated peptide **5** PCS(424–436) was *N*-terminally elongated by three amino acids, Tyr-Asp-Lys. Proteolytic excision-MS again showed only intact uncleaved peptide indicating that Lys and Arg residues are shielded to proteolytic digestion and hence are part of the antibody binding site (Figure 4).

In contrast to the PCS peptide **5**, binding affinity to the antibody was substantially reduced in the short tetrapeptide **14** PCS(427–430-TyrNO_2) lacking basic *N*-terminal amino acids (Figure 5). Trypsin cleavage of **5** prior to antibody binding provided uninhibited cleavage at the *N*-terminal Lys and Arg residues, and yielded reduced antibody binding (data not shown). In contrast, *C*-terminal elongation of the Tyr-430-nitrated peptide sequence by basic or neutral amino acids – Ser-Leu-Pro – (peptide **15**) had no effect on the antibody binding (Figure 5(B)).

Additional characterization of the antibody-binding specificity and a possible preferential epitope motif was performed with a series of PCS peptides that contained different nitrated tyrosine residues. Three peptides, PCS(79–91), PCS(416–426), and PCS(424–436) containing the nitrated tyrosine residues 83, 421, and 430 were compared for their binding affinity, using the corresponding non-nitrated peptides PCS(416–426) (**2**), (79–91) (**4**), and (424–436) (**6**) as a control. While the non-nitrated peptides did not show any affinity, significant differences were found for the nitrated PCS peptides, with the Tyr-83-nitrated peptide **3**

Journal of PeptideScience

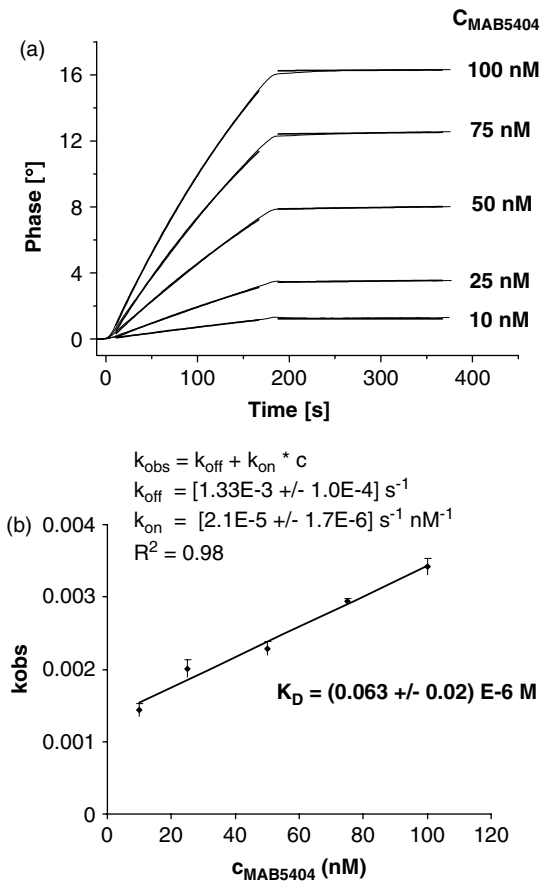

Figure 3. (a) Binding and dissociation curves of the complex of anti nitrotyrosine antibody MAB5404 with the immobilized Tyr430-nitrated peptide **5**; (b) k_{obs} values from the biosensor signals versus antibody concentration, and K_D determination of the immune complex. Antibody concentrations 10–100 nM, and a linear best fit was applied to the data evaluation, providing a K_D of 60 nM.

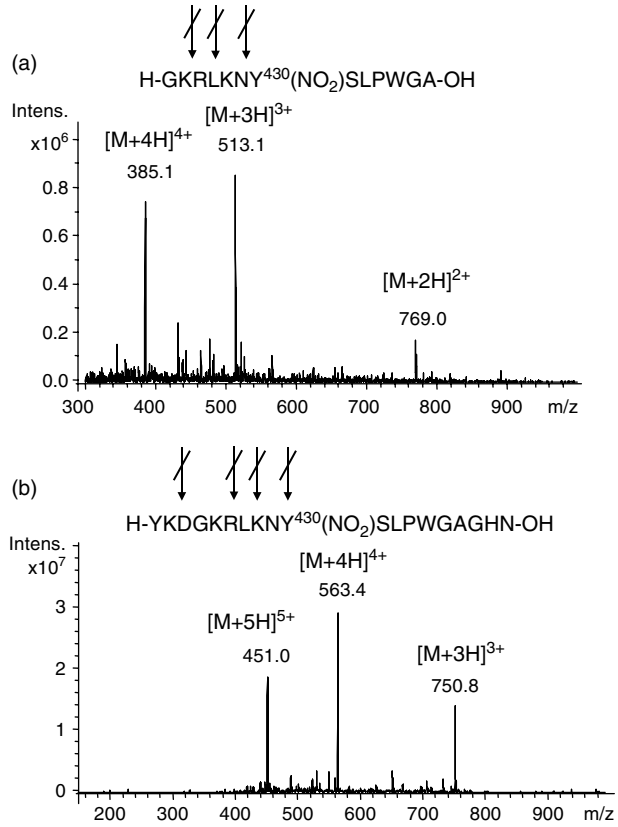

Figure 4. Proteolytic digestion (epitope excision) and MS analysis of immune complexes of MAB5404 antibody with Tyr-430-nitrated PCS peptides. (a) ESI-MS of the elution fraction from proteolytic excision with trypsin of PCS(424–439) **5**; (b) ESI-MS of the elution fraction from proteolytic excision of PCS(421–439) **17**. Tryptic cleavage site (K, R) shielded by the antibody binding are indicated by broken arrows.

PCS(79–91) having the lowest affinity and the Tyr-430-nitrated peptide **5** (424–436) having the highest affinity (Figure 5(B)). These results were consistent with an epitope motif containing positively charged amino acids *N*-terminal to the nitration site.

Discussion

In the present study, we have characterized the affinity and binding specificity of a monoclonal 3-NT-specific antibody to tyrosine-nitrated peptides of PCS which had been previously found to be specifically nitrated *in vivo* at the Tyr-430 residue [17]. The comparison of different tyrosine-containing peptides (comprising tyrosine residues 83, 421, 430) showed that high affinity was not merely dependent on a single nitrated tyrosine residue, but comprised an epitope motif with positively charged neighboring amino acids (Lys and/or Arg) *N*-terminal to the tyrosine nitration site. High antibody binding was found with basic (Lys, Arg) amino acids located at a distance of 2–3 residues from the nitrated tyrosine. However, basic amino acids directly adjacent to the nitration site, or basic residues *C*-terminal to the nitration site did not provide increased antibody binding, suggesting some spatial extension is required for the binding structure. In contrast, neutral or negatively charged residues at the *N*-terminal neighboring peptide sequence showed considerably lower affinity.

A preliminary epitope motif derived from the antibody-binding affinities of the tyrosine-nitrated PCS peptides is shown in Figure 6. In addition to the characterization of sequence variations of PCS(424–426), a comparison of this motif with sequences at tyrosine nitrations recently identified in physiological proteins of eosinophile granules [22] reveals remarkable similarities (Figure 6(B)), suggesting that (i) stabilization by adjacent positively charged residues and (ii) surface exposition of tyrosine-nitrated sites are important factors [7,22]. It should be pointed out that the present data can provide only a preliminary characterization of a tyrosine-nitration motif in proteins. It will be of interest in future studies to evaluate and characterize a possible 'nitration epitope' as a potential oxidative biomarker.

Acknowledgements

This work has been supported by the Deutsche Forschungsgemeinschaft, Bonn, Germany (FOR-753; PR-175-14/1). We thank David Andreu, Pompeu Fabra University Barcelona, and Michael Gross, Washington University St Louis, for helpful discussions on biochemistry of tyrosine nitration and methodology of identification of nitrations, and Thomas Gronewold, Bonn, for technical assistance with the SAW biosensor technology.

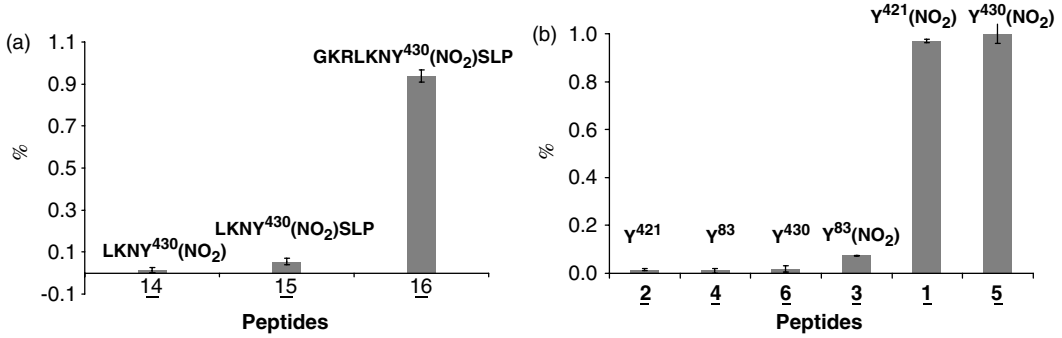

14 H-[427]LKNY[430](NO$_2$)-NH$_2$

15 H-[427]LKNY[430](NO$_2$)SLP[433]-OH

16 H-[424]GKRLKNY[430](NO$_2$)SLP[433]-OH

1 H-[416]EKKDFY[421](NO$_2$)KDGKRL[426]-OH

2 H-[416]EKKDFY[421]KDGKRL[426]-OH

3 H-[79]DPHSY[83](NO$_2$)DAVVWEPR[91]-OH

4 H-[79]DPHSY[83]DAVVWEPR[91]-OH

5 H-[424]GKRLKNY[430](NO$_2$)SLPWGA[436]-OH

6 H-[424]GKRLKNY[430]SLPWGA[436]-OH

Figure 5. Comparison of binding affinities of Tyr-nitrated PCS peptides to the MAB5404 antibody determined by ELISA. (A) Binding of Tyr-430-nitrated peptides **14**, **15**, and **16**; (B) binding affinities of PCS peptides **1**, **3**, **5** nitrated at Tyr-421, Tyr-83, and Tyr-430. Corresponding non-nitrated peptides **2**, **4**, and **6** were used as controls. ELISA determinations are presented at a concentration of 5 μM, respectively.

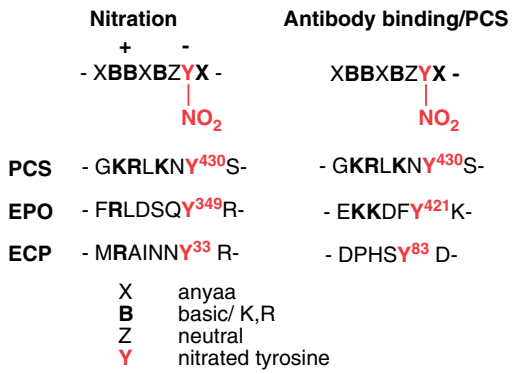

Figure 6. Epitope recognition motif of the nitrotyrosine-specific MAB5404 antibody derived from Tyr-nitrated PCS peptides (right), and nitration sites identified for PCS, eosinophil peroxidase (EPO), and eosinophil-cationic protein (ECP) (left).

References

1 Beckman JS, Ye YZ, Anderson SR, Chen J, Accavitti MA, White CR. Extensive nitration of protein tyrosines in human atherosclerosis detected by immunohistochemistry. *Bio. Chem. Hoppe-Seyler* 1994; **375**: 81–88.

2 Cromheeke KM, Kockx MM, De Meyer GR, Bosmans JM, Bult H, Beelaerts WJ, Vrints CJ, Herman AG. Inducible nitric oxide synthase colocalizes with signs of lipid oxidation/peroxidation in human atherosclerotic plaques. *Cardiovasc. Res.* 1999; **43**: 744–754.

3 Teunissen CE, de Vente J, Steinbusch HW. Biochemical markers related to Alzheimer's dementia in serum and cerebrospinal fluid. *Neurobiol. Aging* 2002; **23**: 458–508.

4 Giasson BI, Duda JE, Murray IVJ, Chen Q, Souza JM, Hurtig HI, Ischiropoulos H, Trojanowski JQ, Lee VM. Oxidative damage linked to neurodegeneration by selective alpha-synuclein nitration in synucleinopathy lesions. *Science* 2000; **290**: 985–989.

5 Beckman JS, Chen J, Crow JP, Ye YZ. Reactions of nitric oxide, superoxide and peroxynitrite with superoxide dismutase in neurodegeneration. *Prog. Brain Res.* 1994; **103**: 371–380.

6 Beckman JS. Oxidative damage and tyrosine nitration from peroxynitrite. *Chem. Res. Toxicol.* 1996; **9**: 836–844.

7 Ischiropoulos H. Protein tyrosine nitration – an update. *Arch. Biochem. Biophys.* 2009; **484**: 117–121.

8 Ryberg H, Caidahl K. Chromatographic and mass spectrometric methods for quantitative determination of 3-nitrotyrosine in biological samples and their application to human samples. *J. Chromatogr. B Analyt. Technol. Biomed. Life Sci.* 2007; **851**: 160–171.

9 Tsikas D. A critical review and discussion of analytical methods in the l-arginine/nitric oxide area of basic and clinical research. *Anal. Biochem.* 2008; **379**(2): 139–163.

10 Tsikas D. Analytical methods for 3-nitrotyrosine quantification in biological samples: the unique role of tandem mass spectrometry. *Amino Acids* 2010; (in press), DOI: 10.1007/s00726-010-0604-5.

11 Franze T, Weller MG, Niessner R, Poschl U. Comparison of nitrotyrosine antibodies and development of immunoassays for the detection of nitrated proteins. *Analyst* 2004; **129**: 589–596.

12 ter Steege J, Buurman W, Arends JW, Forget P. Presence of inducible nitric oxide synthase, nitrotyrosine, CD68, and CD14 in the small intestine in celiac disease. *Lab. Invest.* 1997; **77**: 29–36.

13 Hinson JA, Michael SL, Ault SG, Pumford NR. Western blot analysis for nitrotyrosine protein adducts in livers of saline-treated and acetaminophen-treated mice. *Toxicol. Sci.* 2000; **53**: 467–473.

14 Duda JE, Giasson BI, Chen Q, Gur TL, Hurtig HI, Stern MB, Gollomp SM, Ischiropoulos H, Lee VM, Trojanowski JQ. Widespread nitration of pathological inclusions in neurodegenerative synucleinopathies. *Am. J. Pathol.* 2000; **157**: 1439–1445.

15 Franze T, Weller MG, Niessner R, Poschl U. Enzyme immunoassays for the investigation of protein nitration by air pollutants. *Analyst* 2003; **128**: 824–831.

16 Petre BA, Youhnovski N, Lukkari J, Weber R, Przybylski M. Structural characterisation of tyrosine-nitrated peptides by ultraviolet and infrared matrix-assisted laser desorption/ionisation Fourier transform ion cyclotron resonance mass spectrometry. *Eur. J. Mass Spectrom.* 2005; **11**: 513–518.

17 Schmidt P, Youhnovski N, Daiber A, Balan A, Arsic M, Bachschmid M, Przybylski M, Ullrich V. Specific nitration at Tyrosine-430 revealed by high resolution mass spectrometry as basis for redox regulation of bovine prostacyclin synthase. *J. Biol. Chem.* 2003; **278**: 12813–12819.

18 Stefanescu R, Iacob RE, Damoc EN, Marquardt A, Amstalden E, Manea M, Perdivara I, Maftei M, Paraschiv G, Przybylski M. Mass spectrometric approaches for elucidation of antigen-antibody recognition structures in molecular immunology. *Eur. J. Mass Spectrom.* 2007; **13**: 69–75.

19 Hager-Braun C, Tomer KB. Determination of protein-derived epitopes by mass spectrometry. *Expert Rev. Proteomics* 2005; **2**: 745–755.
20 McLaurin J, Cecal R, Kierstadt ME, Tian X, Phinney AL, Manea M, French JE, Lambermon MH, Darabie AA, Brown ME, Janus C, Chishti MA, Horne P, Westaway D, Fraser PE, Mount HT, Przybylski M, St. George-Hyslop P. Therapeutically effective antibodies against amyloid-beta peptide target amyloid-beta residues 4–10 and inhibit cytotoxicity and fibrillogenesis. *Nature Med.* 2002; **8**: 1263–1269.
21 Macht M, Marquardt A, Deininger SO, Damoc E, Kohlmann M, Przybylski M. "Affinity-proteomics": direct protein identification from biological material using mass spectrometric epitope mappping. *Anal. Bioanal. Chem.* 2004; **378**: 1102–1112.
22 Ulrich M, Petre A, Youhnovski N, Promm F, Schirle M, Schumm M, Pero RS, Doyle A, Checkel J, Kita H, Thiyagarajan N, Acharya KR, Schmid-Grendelmeier P, Simon HU, Schwarz H, Tsutsui M, Shimokawa H, Bellon G, Lee JJ, Przybylski M, Doring G. Post-translational tyrosine nitration of eosinophil granule toxins mediated by eosinophil peroxidase. *J. Biol. Chem.* 2008; **283**: 28629–28640.
23 Drăguşanu M, Petre BA, Slămnoiu S, Vlad C, Tu T, Przybylski M. On-line bioaffinity-electrospray mass spectrometry for simultaneous detection, identification and quantification of protein-ligand interactions. *J. Am. Soc. Mass Spectrom.* 2010; **21**: 1643–1648.
24 Gronewold TM. Surface acoustic wave sensors in the bioanalytical field: recent trends and challenges. *Anal. Chim. Acta* 2007; **603**: 119–128.
25 Andra J, Bohling A, Gronewold TM, Schlecht U, Perpeet M, Gutsmann T. Surface acoustic wave biosensor as a tool to study the interaction of antimicrobial peptides with phospholipid and lipopolysaccharide model membranes. *Langmuir* 2008; **24**: 9148–9153.
26. Petre BA, Dragusanu M, Przybylski M. Molecular recognition specificity of anti-3-nitrotyrosine antibodies revealed by affinity-mass spectrometry and immunoanalytical methods. In *Applications of Mass Spectrometry in Life Safety*. Popescu C, Zamfir AD, Dinca N (eds.). Springer Science: 2008; 55–67.

